Development of a Method for the High-Throughput Quantification of Cellular Proteins

Paolo Paganetti,[a] Andreas Weiss,[a] Monique Trapp,[a] Ina Hammerl,[a] Dorothée Bleckmann,[a] Ruth A. Bodner,[b] Shanie Coven-Easter,[b] David E. Housman,[b] and Christian N. Parker*[a]

The quantification of cellular proteins is essential for the study of many different biological processes. This study describes an assay for the detection of the intracellular mutant huntingtin, the causative agent of Huntington's disease, with a method that may be generally applicable to other cellular proteins. A small recombinant protein tag that is recognized by a pair of readily available, high-affinity monoclonal antibodies was designed. This tag was then added to an inducible fragment of the mutant huntingtin protein by genetic engineering. We show that it is possible to use time-resolved FRET to detect low intracellular levels of huntingtin by a simple lysis and de-tection procedure. This assay was then adapted into a homo-geneous, miniaturized format suitable for screening in 1536-well plates. The use of time-resolved FRET also permits the assay to be multiplexed with a standard readout of cell toxicity, thus allowing the identification of conditions causing reduction of protein levels simply due to cytotoxicity. The screening re-sults demonstrated that the assay is able to identify com-pounds that modulate the levels of huntingtin both positively and negatively and that represent valuable starting points for drug discovery programs.

Introduction

Huntington's disease (HD) is a fatal, autosomal-dominant neu-rological disorder. The disease is characterized by involuntary movements, severe emotional disturbance, and cognitive de-cline caused by a considerable degeneration of brain matter.[1] In 1993, the gene IT15 was found to contain a CAG repeat ex-panded in patients and encoding for a polyglutamine (polyQ) track located at the amino terminus of the huntingtin (Htt) protein.[2] A number of possible effects of this longer mutated polyQ sequence on cell physiology have been suggested, in-cluding the generation of cytotoxic proteolytic fragments and aggregates, transcriptional dysfunctions, and several other ef-fects. Currently, there are no approved disease-modifying treat-ments for HD.[3]

Even though the mechanism of mutant Htt toxicity is un-known, it has been shown in mouse models that down-regula-tion of mutant Htt expression by RNA interference[4] or by con-ditional expression[5] significantly improves HD-like symptoms. Furthermore, compounds that affect Htt aggregation have been shown to reverse Htt toxicity.[6] Critically, mutant and normal Htt present different post-translational modifications, such as phosphorylation,[7] proteolytic cleavages,[8] cellular lo-calization,[9] or degradation by autophagy or by the ubiquitin/proteasome pathway.[10] Because mutant Htt is the sole cause of HD and because the cell metabolizes mutant and normal Htt differently, we established an assay capable of detecting the intracellular levels of wild-type or mutant Htt. In order to develop this assay, neuronal cell lines with inducible copies of either the wild-type or mutant Htt tagged with small peptide sequences were created and a method for the detection of compounds that promote Htt degradation was developed.

In general, most methods for monitoring of cellular protein levels require separation and detection steps, such as Western blot, ELISA, or HPLC–MS. Such methods are not suitable for testing of multiple conditions—that is, high-throughput screening of chemicals and siRNAs—because those applica-tions require homogeneous assays that are robust enough to allow automation. To circumvent these problems, we devel-oped an alternative method based on time-resolved Förster resonance energy transfer (time-resolved FRET), a technology that has been available for monitoring biomolecular interac-tions since the early 1990s.[11] There are many different applica-tions of this technology, utilizing several aspects of the fluores-cence characteristics of lanthanoid ions. The large Förster's dis-tances of the rare earth ions are up to 9 nm; this is much larger than for many fluorescent compounds, which have För-ster's distances of 4–6 nm. Absorbed energy is therefore trans-ferred over much longer distances than for other FRET pairs, so it is advantageous to use rare earth chelates as generic im-

[a] Dr. P. Paganetti,+ Dr. A. Weiss,+ M. Trapp, I. Hammerl, D. Bleckmann, Dr. C. N. Parker
Novartis Institutes for Biomedical Research Basel,
Novartis Pharma AG
WKL-125.7.19, 4002 Basel (Switzerland)
E-mail: paolo.paganetti@novartis.com

[b] Dr. R. A. Bodner, S. Coven-Easter, Prof. D. E. Housman
David H. Koch Institute for Integrative Cancer Research
Massachusetts Institute of Technology
Cambridge, Massachusetts (USA)

[+] These authors contributed equally to this work.

Supporting information for this article is available on the WWW under http://dx.doi.org/10.1002/cbic.200900131.

munodetection reagents.[12] The second advantage of rare earth FRET is that the time it takes for the fluorescence to decay is greatly extended, thus allowing time-resolved fluorescence measurement. The effect of this is to reduce the influence of short-lived background fluorescence from small molecules being tested. The third advantage is the potential for monitoring of ratiometric readouts—that is, the emission of the lanthanoid ion over that of the FRET-coupled fluorophore—which reduces assay variability and improves data quality.[13]

Time-resolved FRET has therefore been used in the past to monitor a number of different biological analytes such as small molecules (cAMP, for example[14]) or small secreted cytokines (IL-8, for example[15]), as well as the levels of phosphorylated proteins in in vitro assays.[16] There have also been reports of the use of time-resolved FRET to monitor the levels of phosphorylated proteins in cell lysates through the use of cell lines that overexpress protein substrates of interest.[17] In this report we have extended these observations by designing a small peptide tag that gives an optimal time-resolved FRET signal and allows the detection of mutant Htt expressed at low intracellular levels. Because the Htt detection in this assay is based on an artificial tag, this method should be generally applicable for the detection of other proteins. Importantly, the required antibody pairs for tag detection are commercially available, and this makes our method a readily applicable generic detection technology for other laboratories.

Results

Technology development

A time-resolved FRET detection assay based on two high-affinity antibodies directed towards well-characterized epitopes in the amyloid Aβ peptide has been described[18] and is currently commercially available. We reasoned that by taking advantage of this knowledge we might be able to design a generic tag for homogenous protein detection by time-resolved FRET through the utilization of a small peptide to which two commercially available and high-affinity Aβ peptide monoclonal antibodies would bind simultaneously. Because FRET efficiency can be influenced by various parameters,[19] we generated a library of small peptides (Figure 1 A) containing the two Aβ peptide epitopes EFRH and GGVV, in which length and amino acid composition of the linker were varied to determine the optimal tag sequence. A repeated GGS sequence was chosen to build the linker, to provide favorable flexibility and linearity between the epitopes. Time-resolved FRET detection with the purified peptides and the antibody pair 25H10K and β1-d2 showed that linker length and peptide sequence can indeed influence signal intensity significantly (Figure 1 B). Peptides with very short linker lengths (peptides H2 and H3), for example, gave weak signals, probably due to steric hindrance between the two antibodies. The strongest time-resolved FRET signal was obtained with the peptide H1, in which the two four-amino-acid epitopes of the Aβ peptide were separated by a linker of 12 amino acids. Peptide I6, in which the neo-epitope GGVV for
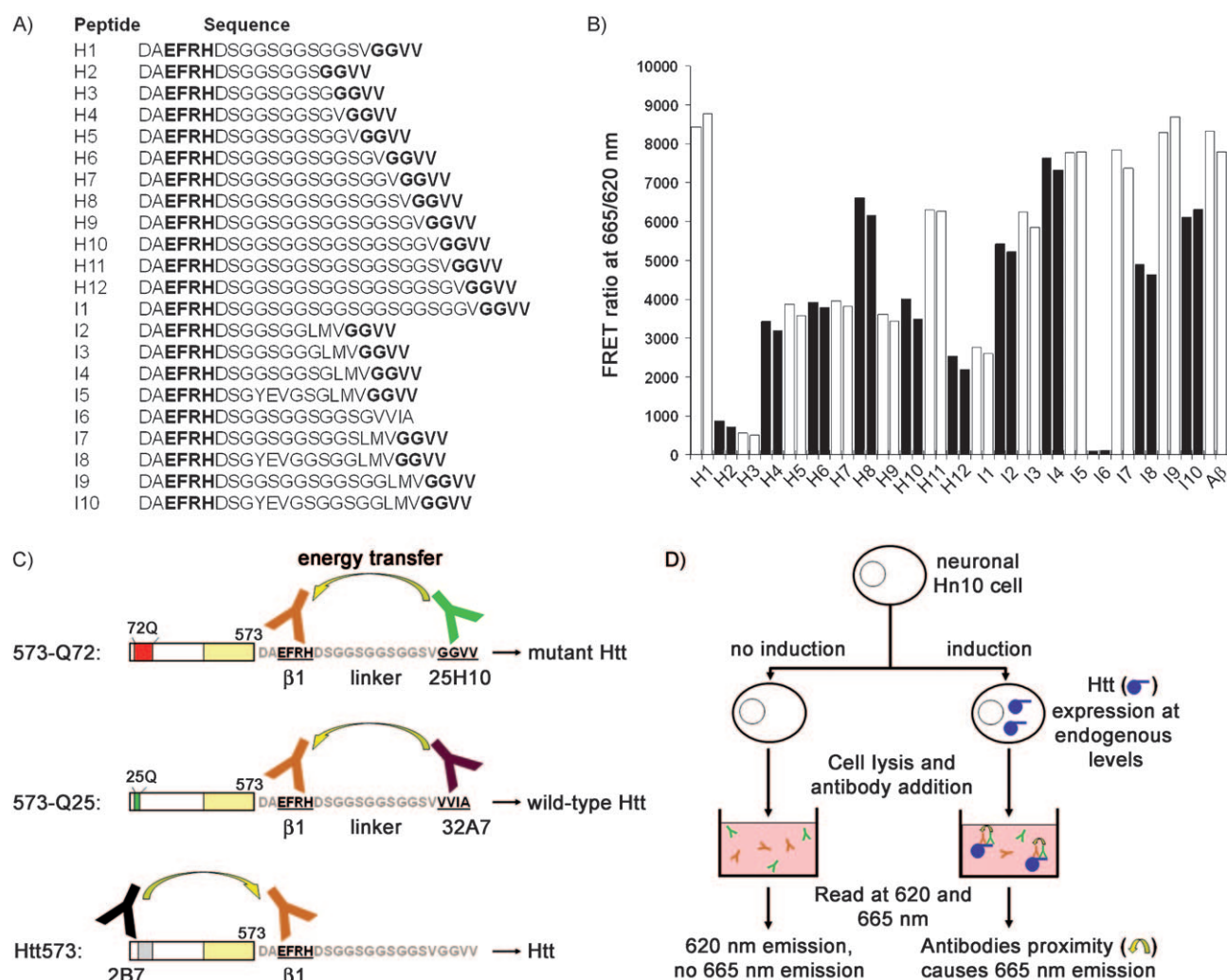
the 25H10 antibody was replaced by VVIA, specific for the 32A7 antibody, was not detected by the 25H10K and β1-d2 pair, thus verifying the specificity of the assay.

For further experiments we designed two Htt fragments carrying either the exact H1 peptide sequence as a tag for mutant Htt (Htt573-Q72) or the alternative sequence of peptide I6 for wild-type Htt (Htt573-Q25) (Figure 1 C). The protein fragments each encompassed the first 573 amino acids of human Htt and thus contained several sites known to be posttranslationally modified in the HD brain. These constructs were stably transfected in neuronal HN10 cells; this created three cell lines with inducible expression variously of mutant Htt, of wild-type Htt, or of a combination of mutant and wild-type Htt. These cell lines were utilized to establish a high-throughput time-resolved FRET assay for detection of intracellular Htt protein (Figure 1 D).

Protein detection and signal specificity

The neuronal clonal cell lines expressed the tagged mutant Htt and wild-type Htt at levels corresponding to that of endogenously expressed Htt upon full induction, with no detectable basal expression as demonstrated by Western blot analysis (Figure 2 A). Expression levels of the constructs were stable over time and cell passages (Figure 2 B). Experiments with a 96-well plate format showed that highly specific time-resolved FRET detection either of the wild-type or of the mutant Htt was feasible in a cellular context when using the antibody pairs 25H10K and β1-d2 or 32A7K and β1-d2 that specifically detected their corresponding tags. In addition, use of the 2B7K antibody specific for an amino-terminal endogenous Htt epitope in combination with the β1-d2 antibody specific for an epitope in the carboxy terminal tag allowed for selective detection of noncleaved Htt (Figure 2 C) in the cell lines expressing either wild-type or mutant Htt.

In order to determine the maximum level of Htt expression in the HN10 cells, we first calibrated our assay by using increasing concentrations of peptide H1 diluted into cell lysates from noninduced cells (Figure S1 in the Supporting Information). We determined the linear range of the time-resolved FRET assay and so calculated an amount of mutant Htt corresponding to 17 ng per mg total HN10 protein, based on the assumption that the synthetic H1 peptide and tagged Htt generate similar time-resolved FRET signals with the antibody pair 25H10K and β1-d2. These data demonstrated that although Htt is expressed at relatively low levels in HN10 cells, the intracellular concentration of mutant Htt was significantly higher than the detection limit of the assays (3.6 ng mutant Htt per mg total cellular protein) calculated as threefold standard deviation over the background signal. Interestingly, replacement of the 25H10 antibody specific for the epitope GGVV of peptide H1 with the 32A7 antibody specific for the VVIA epitope significantly improved the dynamic range of the assay when peptide I6 was used (Figure S1), possibly because of a difference either in the affinity constants of the two antibodies or in the conformation of the two protein tags. As would be expected, when the 32A7 antibody was utilized in the time-resolved FRET assay,

Figure 1. Optimization of detection tags, cDNA constructs and assay principle. A) Amino acid sequences of peptides analyzed with the antibody pair 25H10K and β1-d2 are shown, with the corresponding epitopes in bold letters. B) Time-resolved FRET analysis of peptides (3 ng per well in duplicates) shown in A). The H1 sequence was selected for tagging mutant Htt and the I6 sequence was selected for tagging wild-type Htt. C) Schematic representations of cDNA constructs expressed in the inducible HN10 cell lines; also indicated are the antibody binding sites of 25H10 (green), 32A7 (purple), and β1 (orange) in the C-terminal tag. 2B7 (black) detects an endogenous N-terminal epitope of Htt. D) Schematic representation of the protocol used for the cell-based time-resolved FRET assay.
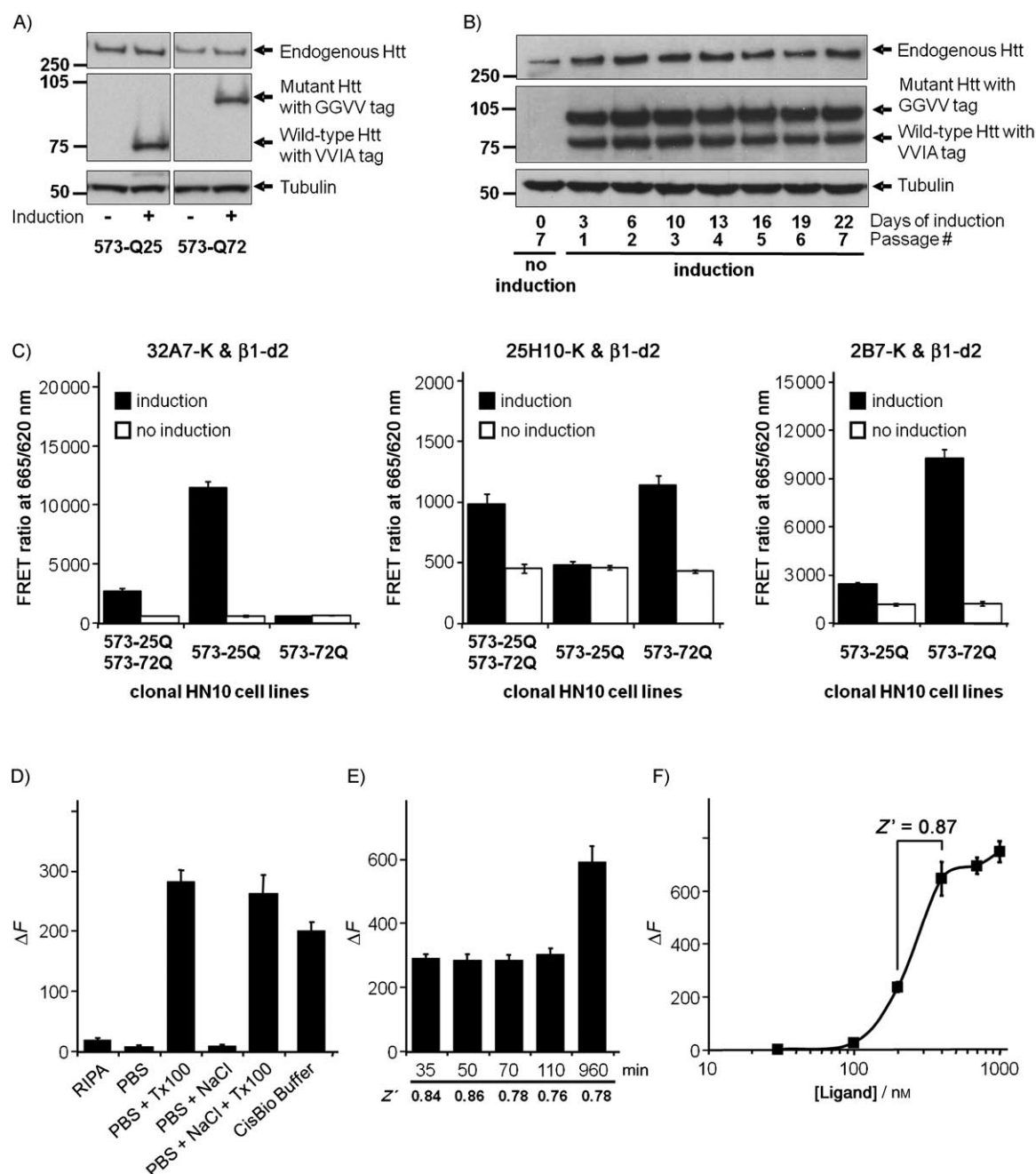
all other peptides carrying the GGVV epitope were not detected (data not shown).

Assay miniaturization

We proceeded to miniaturize the assay to a 1536-microwell plate format. Because we have the capacity to retest thousands of compounds in dose-response manner, we decided first to use the detection of mutant Htt in the Htt573-Q72-expressing HN10 cells as readout for the HTS. If necessary, positive compounds could then be counter-screened on wild-type Htt cells. This strategy allowed the use of the 2B7K and β1-d2 antibody pair (Figure 1C), which not only generated a large dynamic range when measuring Htt (Figure 2C), but also allowed for monitoring of possible effects of the compounds on the total amount of Htt present in the cells, as well as on the cleavage of the intact Htt.

The optimal cell density in the 1536-microwell plate was established in a cell dilution experiment. We observed a linear relationship between cell number and the amount of Htt measured by time-resolved FRET (data not shown), with approximately 6000 to 8000 cells per well judged optimal for the HTS assay (see also below).

Steady-state levels of Htt expression (wild-type and mutant) were reached after three days of induction with RSL-1 (400 nM, Figure 2B). For the HTS assay, the Htt573-Q72-expressing HN10 cell line was therefore preincubated in inducing medium for 72 h to express mutant Htt, after which the cells were seeded in the 1536-well plates. The level of background signal was determined from wells containing noninduced cells (that is, cells in the absence of the RSL1 inducer or any other additives). Steady-state Htt expression required the continuous presence of the RSL1 inducer, but we were able to establish that an overnight incubation in the absence of the ligand resulted in

Figure 2. Detection of mutant and wild-type Htt by time-resolved FRET. A) Western blot analysis of RSL-1-induced (400 nM) expression of wild-type (573-Q25) and mutant (573-Q72) Htt in HN10 cells relative to that of endogenous full-length Htt. B) After three days of induction with RSL-1 (400 nM), the HN10 cell line transfected with mutant and wild-type Htt shows stable Htt expression over time and multiple cell passages. C) Sensitive and specific detection of wild-type or mutant Htt by time-resolved FRET with use of the indicated antibody combinations [RSL-1 (400 nM) induction for three days (average value, $n = 3$, standard deviation)]. D) Optimization of cell lysis conditions for detection of mutant Htt573-Q72 in cells induced for three days with RSL-1 (400 nM) and use of the 2B7 and β1 antibody pair (time-resolved FRET measured 50 min after antibody addition, $n = 6$, standard deviation). E) The Z'-factor remained stable between 35 and 110 min after cell lysis and addition of the detecting antibodies, although the absolute time-resolved FRET signal increased over time (not shown) [RSL-1 (400 nM) induction for three days of 573-Q72 HN10 cells ($n = 6$, standard deviation)]. F) Dose-dependent increase in mutant Htt573-Q72 expression in cells treated with different RSL1-inducer concentrations ($n = 6$, standard deviation, EC50 ~ 250 nM). A–C) The data were generated in 96-well plate format. D–F) The data were generated in 1536-well plate format.

about fivefold reduction in mutant Htt (data not shown). Htt clearance is a consequence of an unidentified degradation mechanism used by HN10 cells. A goal of this project was the identification of low-molecular-weight modulators of this process. Based on these observations, we opted to assess the
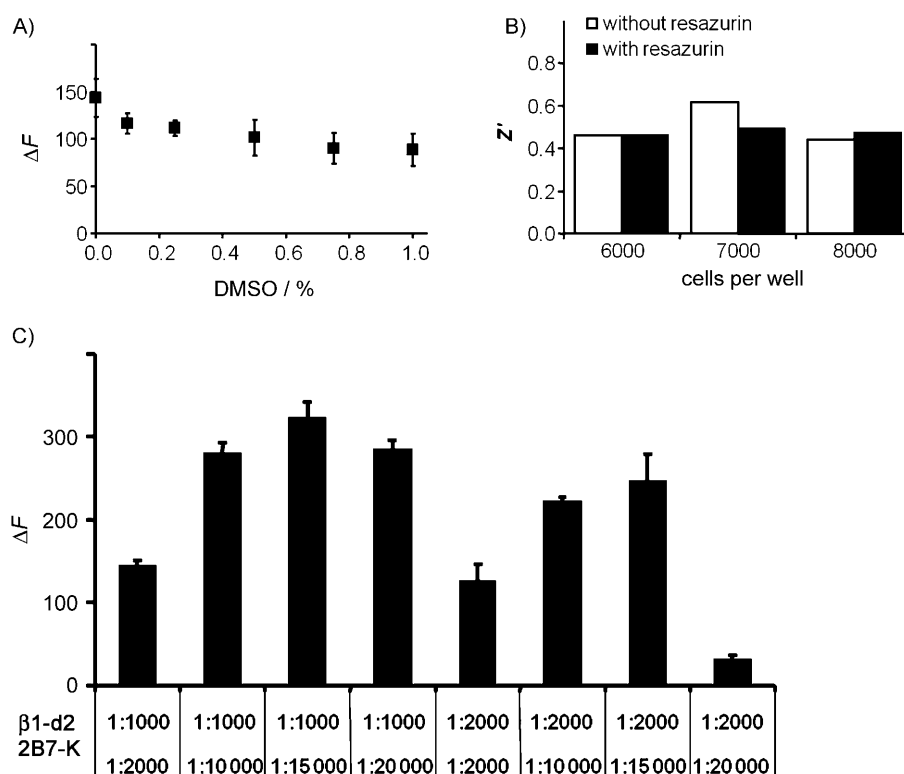
effect of the test compounds in the HTS assay after an overnight (16–18 h) incubation time.

After miniaturization of the format to cells grown directly in a 1536-microwell plate, the assay protocol was optimized for lysis buffer and signal development over time (Figure 2D).

From these optimization experiments, the lysis buffer selected for the HTS was PBS containing Triton X100 (0.4%). Overall, the ΔF values obtained with the 1536-well format were lower than those obtained during assay development. The 1536-well format experiments were conducted as similarly to the screening conditions as possible, so the plates were read on the ViewLux™ whole-plate imager and not with the EnVision® single-well reader used during assay development; this explains this drop in ΔF values. Even though induced-to-noninduced signal ratio improved as a function of incubation time, the Z'-factor had already reached a maximum of 0.86 after a shorter incubation time and remained constant for the time period between 0.5 and 2 h after cell lysis (Figure 2E); this shows that, once the system had reached equilibrium, the assay signal was stable. This observation was important, because it indicated that the time necessary for the assay plates to be processed was not limited by the speed of the reader, and hence on the number of assay plates processed in a batch. Detection optimization progressed with determination of the minimum concentration of inducer required for maximum expression. Mutant Htt expression showed a good response to changing inducer concentrations (Figure 2F), with an EC_{50} corresponding to 0.25 μM and a Z'-factor of 0.87 between signals at 400 nM and 200 nM inducer; this shows the reliability of the assay for a partial ($\sim 50\%$) reduction in mutant Htt.

Figure 3 presents some of the additional assay validation steps taken to characterize the 1536-well assay. Firstly, the DMSO tolerance of the assay was tested to ensure that DMSO, which was used as the compound solvation agent, did not affect the assay signal by altering cell growth or interfering with the readout (Figure 3A). DMSO was tolerated well up to a concentration of 1%, which is above the maximum concentration of 0.5% DMSO that is normally accepted in-house for a cell-based HTS campaign. ANOVA analysis by the Tukey–Kramer multiple comparisons test (InStat version 3.01) showed that the 0% DMSO conditions were not significant in comparison with 0.1% DMSO ($P > 0.05$), but were significant in relation to the other treatments ($P < 0.05$). A significant difference between the conditions with different DMSO concentrations was only noted at 0.75% and 1% ($P < 0.05$) relative to 0.1, 0.25, and 0.5%. Test compounds were diluted 400-fold, starting from

Figure 3. Optimization of HTS assay conditions. A) Effect of increasing DMSO concentrations on expression and time-resolved FRET signal (1536-well plate format, standard deviation). B) Z'-factor values at different cell densities in cell-based assays run in the presence or absence of resazurin as a cell viability assay. The raw data from at least 48 wells were considered when generating the mean and standard deviation values used in the Z'-factor calculation (1536-well plate format). C) Optimization of 2B7 and β1 antibody concentration for Htt detection in induced HN10 cells by time-resolved FRET (1536-well plate format, standard deviation).

90% DMSO stock solution for the HTS, so the effective concentration during the compound incubation was below 0.25% DMSO. To calculate the no-effect values, each plate contained wells with induced cells but treated with a matched DMSO concentration in the incubation medium. The effect of cell density on the assay robustness was determined by assessing the Z'-factor (with induced and noninduced cells as high and low controls, respectively), which remained constant over a range between 6000 and 8000 cells per well (Figure 3B). Since unbound europium cryptate-labeled antibody can contribute to unspecific background signal in time-resolved FRET assays, it was important to select the most appropriate dilutions of the two monoclonal antibodies used in the assay. An example of optimization of antibody concentrations is shown in Figure 3C. We paid attention to selecting the highest dilution of the antibodies that did not result in a drop in the dynamic range of the time-resolved FRET—that is, above 1:1000 for the β1-d2 and above 1:15000 for the 2B7K antibody. From this, we selected an antibody concentration corresponding to 60 pg per well (1:15000) 2B7K and 800 pg per well (1:1000) β1-d2 for the HTS. As a general rule, we observed that the time-resolved FRET readout calculated as the ratio of the d2 emission at 655 nm over the K emission at 620 nm can be significantly reduced by a bleed-through of excessive K fluorescence into the d2 emission channel. The maximum dynamic range can thus

only be obtained by carefully diluting the two antibodies to optimum concentrations at which unwanted bleed-through is minimized while the antibodies are still applied at saturating concentrations.
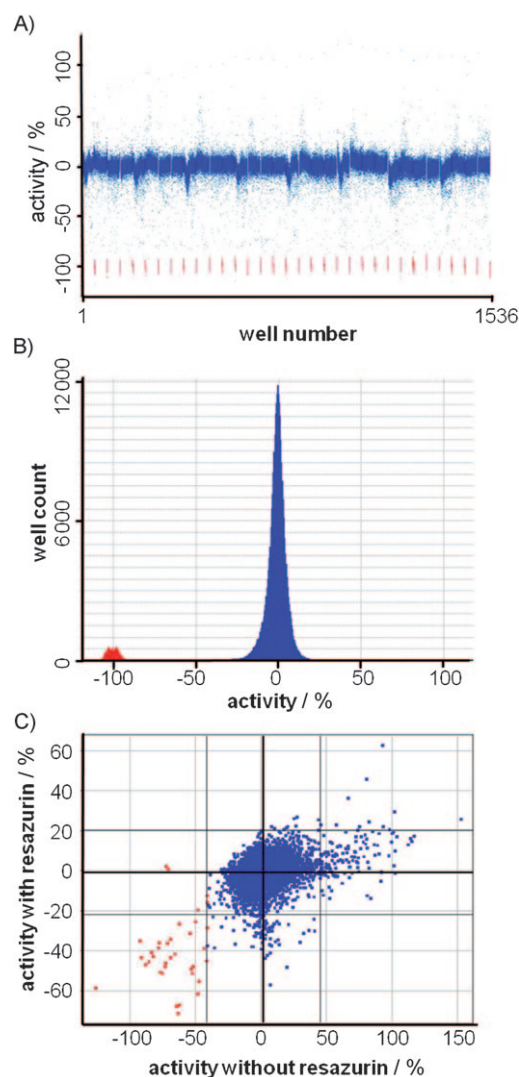
High-throughput screening

The miniaturized assay was applied to screening of a small library composed of ~10 000 compounds commonly used in-house for validation of an assay performance under real HTS conditions before commencement of screening of the full-deck library. In addition, because no compound that specifically reduces mutant Htt expression in cells is known, the primary hits may find use as reference compounds for screening of the full-deck compound collection. Analysis of the prescreen values demonstrated excellent performance, with Z'-factors averaging ~0.6 over multiple plates. Close inspection of the primary data, however, did show that there was a small but significant "edge effect" in all plates tested in the prescreen. This edge effect was more evident when the correction pattern of the analyzed plates was viewed (data not shown) or when the data for all screening plates were arranged by well number (Figure 4 A). This view showed a regular "saw tooth" pattern due to plate edge effects. However, this effect was only minor and did not affect the statistics of the assay performance much, as shown in Figure 4 B with the primary data presented in a Gaussian distribution.

Comparison of results obtained with resazurin

It was also possible to multiplex Htt detection with a measure of cell viability—the chemical reduction of resazurin by mitochondrial activity.[20] For this, we quantified the reduction of the nonfluorescent blue dye resazurin to its reduced pink fluorescent form resorufin. Since resazurin itself is nontoxic, we added the dye directly to the medium and measured its bioreduction to resorufin; this in turn reflected the metabolic state and general cell viability. After resorufin quantification, cells were lysed and processed for time-resolved FRET determination of mutant Htt.

Multiplexing with the cytotoxicity assay had little influence on the robustness of the assay. This was demonstrated by comparing the assay performance of the standard single readout with the multiplexed assay format by use of a set of the preplated compounds (Figure 4 C). If anything, the data generated by the multiplexed readout showed less variability. Comparison of the compound activity in the two assay formats demonstrated that 90 % of the compounds identified as hits in the single-readout format were also identified in the dual-readout format, with a general compound hit rate of ~0.4 % (activity cut-off: threefold standard deviation over the mean signal), confirming high reproducibility and reliability of the cell-based time-resolved FRET assay. Hits were defined as those compounds showing activity greater than threefold standard deviation from the mean signal. This criterion was used so that a consistent hit selection could be made between different assay readouts (for example, time-resolved FRET determination and

Figure 4. Screening performance. A) Overlay of activity data for multiple 1536-well plates, with the x-axis representing the well number for each plate. This representation facilitates identification of plate edge-effects. B) Frequency distribution of activity data for all the screening plates shows an excellent separation of induced cells in the presence of test compounds (blue) from the positive controls represented by noninduced cells (red). C) Comparison of activity for single test compounds examined for cell viability in the presence or in the absence of resazurin: 90 % of the hits (red) were identified in both assay formats, overall hit rate ~0.4 % under the two sets of test conditions.

resazurin measurement) that may have different variability and sample means.
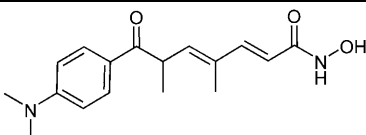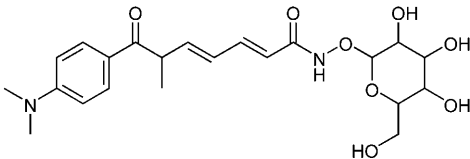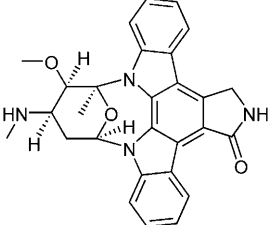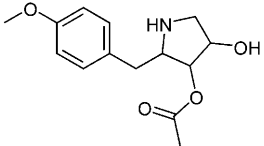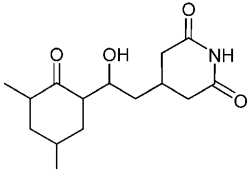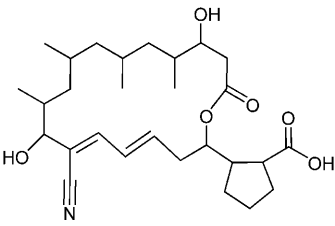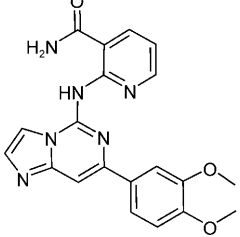
Characterization of active compounds

The Novartis compound archive contains one of the largest collections of purified natural products. Screening of these compounds has the advantage that many of the compounds have previously reported activity and their mechanism of action is known, thus suggesting possible targets involved in the cellular regulation of mutant Htt expression. Screening of this natural product library identified a number of compounds that increased the levels of mutant Htt present in the cells (Fig-

ure S2 in the Supporting Information). Although not the primary focus of this project, these Htt inducers might become interesting research tools because they might help in identification of cellular mechanisms that regulate Htt metabolism and ultimately toxicity.[21] Compounds that increase mutant Htt could, for example, be affecting proteolytic cleavage of Htt, Htt aggregation, or interaction with other proteins.[6] As is often the case when a cell-based HTS is run, many compounds identified will eventually represent false positive hits that disturbed Htt expression or just the detection method by unspecific mechanisms. Indeed, a number of the compound hits that increased Htt expression were chlamydocin or trichostatin A analogues, HDAC inhibitors known to cause general upregulation of gene expression (Table 1).[22]

Table 1. Compounds with known biological mechanisms of action and their activities in the assay.

Compound		Structure	Biology	Activity [%]	
				in assay	in tox. assay
1	trichostatin A analogue		HDAC inhibitor	68	−10
2	trichostatin A analogue		HDAC inhibitor	67	10
3	staurosporine		protein kinase inhibitor	−84	−40
4	anisomycin		protein synthesis inhibitor	−79	−41
5	cycloheximide		protein synthesis inhibitor	−74	−61
6	borrelidin		protein synthesis inhibitor	−73	−35
7	BAY 61-3606		SYK kinase inhibitor	−27	n.d.

n.d. = not determined

Compound hits that effectively lowered mutant Htt expression were clearly more interesting (Figure S2 in the Supporting Information), although these compounds may work by perturbing cell viability or some other unspecific effects. Cycloheximide, borrelidin, and anisomycin, for example, lowered the levels of mutant Htt but also had differing effects on cell viability in this assay. These compounds represents three different classes of general inhibitors of protein synthesis (Table 1).[23] The results presented in Table 1 also show how the multiplexed assay can be used to help prioritize compounds for further evaluation; for instance cycloheximide clearly has a greater effect on cell viability that anisomycin or borrelidin. Other compounds that reduced the intracellular levels of mutant Htt in HN10 cells were a number of staurosporine analogues (unselective protein kinase inhibitors) as well as BAY 61–3606 (a specific syk kinase inhibitor),[24] both known to interfere with various cellular pathways (Table 1).

We validated the time-resolved FRET findings of compound hits that were increasing or reducing Htt in cells by an orthogonal assay: determination of the amount of intracellular Htt present in cell lysates by Western blot. Using both detection methods, we obtained a consistent dose-response effect for a reference compound that decreased Htt levels (cycloheximide, Figure 5 A), as well as for a reference compound that increased Htt expression (trichostatin A analogue, Figure 5 B). The primary hits were also tested on wild-type Htt-expressing HN10 cells, but no specific effect on mutant Htt over wild-type Htt was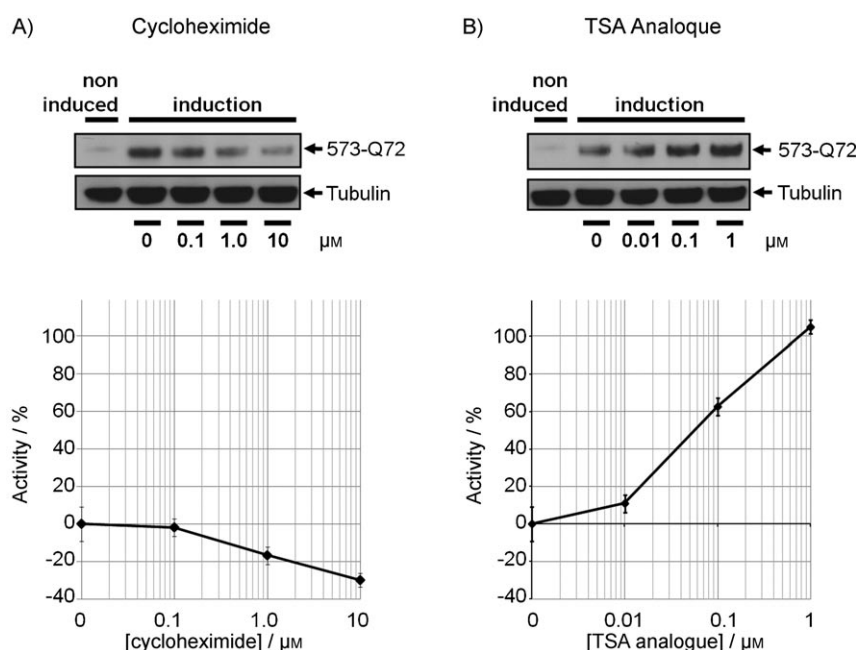 found (data not shown). It should be noted that excellent correlation between the amount of Htt measured by time-resolved FRET and the amount of Htt detected by Western blot was found in many experiments performed by our group, including those shown in Figure 2. These data confirmed that our assay format is suitable for HTS implementation because the time-resolved FRET data were validated by an alternative detection method.

The dynamic response of the assay to compounds with known mechanisms of action, such as the protein synthesis inhibitor cycloheximide or the transcription upregulator trichostatin A, as well as the Western blot validation, demonstrated that our screening assay can be used for the identification of low-molecular-weight modulators of Htt. The possibility of adapting the cell-based assay and readout methodology to automated ultra-throughput screening should advance this technology to the testing of the whole Novartis compound library, and this may result in attractive drug discovery programs for Htt-reducing therapies.

Discussion

This report describes the design and implementation of a time-resolved FRET assay that allows the quantification of proteins, even those expressed at low endogenous levels. The assay format is homogenous and robust enough to allow miniaturization for HTS. The assay represents a method for measuring the steady-state levels of Htt and has been used to identify compounds that modulate the intracellular levels of mutant Htt.

To develop and to validate the detection of intracellular recombinant Htt expressed at low levels, several experimental steps were taken. Firstly, we created a peptide library with peptides displaying two epitopes against well-characterized and commercially available amyloid Aβ antibodies. Since the detection signal of an immune-based time-resolved FRET assay can be influenced by distance and steric orientation of the antibodies, the epitopes were separated by varying linker length to determine the most favorable peptides for detection. We proceeded to use the optimal peptide sequences as generic tags for recombinant Htt constructs and developed neuronal cell lines with inducible expression of tagged Htt at endogenous levels. After verifying the specificity of the time-resolved FRET signal for wild-type or mutant Htt, we carefully tuned the assay

Figure 5. Mutant Htt quantification by Western blot and time-resolved FRET. A) HN10 cells expressing mutant Htt573-Q72 were treated overnight in the presence of increasing amounts of the protein synthesis inhibitor cycloheximide as indicated. After the treatment, cell lysates were collected and analyzed by Western blot with antibody 2B7 or by time-resolved FRET with the 2B7 and β1 antibodies. Cycloheximide caused a consistent dose-dependent decrease in mutant Htt protein as shown by both detection methods. B) The same experiment as shown in A), but with a HDAC inhibitor (TSA analogue) as a generic transcription up-regulating agent. Both Western blot and time-resolved FRET show a consistent dose-dependent increase in mutant Htt expression levels. A–B) Data generated in 96-well plate format ($n = 3$, standard deviation).

conditions to facilitate automated HTS compound screening. We then tested ~10 000 compounds for their ability to modulate intracellular Htt levels, with or without multiplexing with a cytotoxicity readout. This validated both the high reproducibility and the excellent dynamic response of the assay. Further, by screening a library of natural products we identified compounds that could efficiently reduce or augment the amount of mutant Htt present in the cells.

Some caveats with this assay format have to be considered. Firstly, the cell lysis conditions need to be optimized for each set of protein and antibody detection reagents (unpublished observations). Secondly, the assay only detects proteins that are solubilized during cell lysis, which might mean that this format would not be suitable for monitoring the levels of proteins involved in large macromolecular complexes that are not readily solubilized (such as proteins associated with the cell cytoskeleton or the nuclear structure). Thirdly, because of the use of a recombinant peptide tag it is necessary to confirm whether or not a change in signal is indeed reflected in an actual change in protein expression and is not the result of potential proteolysis or other post-translation modifications of the peptide tag, such as phosphorylation or acetylation, which might alter the ability of the antibody to bind to the recombinant tag. The peptide tag might also affect function, folding, or clearance of the protein being studied. Fourthly, whereas it is possible to multiplex Htt detection with an assay to monitor cell viability, the current assay setup uses a measure of mitochondrial redox potential that may not be sensitive enough to detect unspecific changes in cell physiology altering protein expression, and this readout indeed has a tendency to underestimate the potential cytotoxicities of compounds (data not shown). However it is still possible to multiplex Htt detection with additional cytotoxicity readouts such as ATP levels or even other reporter gene assays.

One advantage of this tagging approach is that, in addition to the biochemical quantification of the protein, it is possible to adapt the format for protein visualization in intracellular imaging assays with use of fixed and permeabilized cells. This would allow monitoring not only of the levels of protein during a change in conditions but also of the location of the protein within the cell. In the case of Htt this is of importance because it has been reported that intracellular localization of Htt influences its toxicity[1,25] and might also have a bearing on the apparent protein levels.[26]

The basic strategy applied in this study for the high-throughput detection of tagged proteins can be extended to assays that use antibodies to nonrecombinant epitopes, and this would allow the detection and quantification of endogenous proteins.

Experimental Section

Peptides and antibodies: A library of peptides carrying epitopes recognized by the monoclonal antibodies 25H10, β1, or 32A7 was custom-produced by MIT Biopolymers Laboratory (MIT, Cambridge, MA, USA). Amyloid Aβ40 peptide was purchased from Bachem (Bubendorf, Switzerland).

The 25H10 antibody specific against the GGVV epitope, the 32A7 antibody specific against VVIA, and the β1 antibody directed against EFRH are described elsewhere.[27] The EFRH epitope of human amyloid Aβ peptide is not present in the corresponding mouse polypeptide, so no background detection of amyloid Aβ peptide expressed by mouse HN10 cells is possible. Commercially available unlabeled antibodies equivalent to these antibodies can be obtained through several vendors such as Cell Sciences (Canton, MA, USA), The Genetics Company AG (Schlieren, Switzerland) or Immuno-Biological Laboratories (Minneapolis, MN, USA). Labeled antibodies ready for time-resolved FRET can be obtained through Cisbio Bioassays (Bagnols-sur-Cèze, France). The 2B7 antibody was custom designed against the first 17 amino acids of Htt (GENOVAC, Freiburg, Germany). Custom europium cryptate (K) and d2-fluorophore (d2) labeling was performed by Cisbio Bioassays. Depending on the batch, antibodies were cross-linked to 5–7 mol of K or d2 per mol antibody.

Generation of neuronal cell lines: Neuronal HN10 cells[28] were used to create inducible clones with expression of Htt573-Q25 and/or Htt573-Q72. In brief, cells were transfected with the Rheo-Switch receptor plasmid pNEBR-R1 (New England Biolabs) and cultured under selection of G418 (1 mg mL^{-1}, Invitrogen). Clones were screened for cell morphology, transfected with inducible luciferase reporter construct, and induced for two days. The clone with the best induction ratio was selected and used for subsequent transfection with Htt573-Q25 or Htt573-Q72 inducible plasmids (in pNEBR-X1Hygro vector). After selection with G418 and hygromycin (1 mg mL^{-1}, Invitrogen), inducible expression of Htt fragments in the clonal lines were monitored by the time-resolved FRET detection method described here, and clones with no basal expression and highest inducible expression were chosen for use in the assay format.

Detection of peptides by time-resolved FRET: Peptides (800 μg mL^{-1}) were dissolved in DMSO. Test peptides and amyloid Aβ40 peptide (3 ng mL^{-1}) were diluted in RIPA buffer [20%, Tris-HCl (10 mM) pH 7.5, NaCl (150 mM), EDTA (1 mM), NP40 (1%), SDS (0.5%)] and Complete Protease Inhibitor (Roche). Peptide solutions (30 pg, 10 μL) in each well were mixed with an antibody solution (5 μL) composed of 25H10K (2 ng) and β1-d2 (20 ng) dissolved in NaH$_2$PO$_4$ (50 mM, pH 7.4, NaF (400 mM), BSA (0.1%), and Tween 20 (0.05%) in a low-volume 96-well plate and incubated at 4 °C overnight. Time-resolved fluorescence at 620 and 665 nm was measured with a RUBYstar (BMG Labtech) reader.

Adaptation to 96-well plate format: Cells were seeded in Dulbecco's modified Eagle's medium (Gibco) growth medium with fetal calf serum (FCS, 10%), penicillin, and streptomycin (20 000 cells per well, 100 μL per well). The medium was removed after 2 h and was replaced with inducing medium (200 μL per well, growth medium plus RSL1 inducer) to start the expression of Htt. After three days, medium was removed and replaced with the readout buffer [30 μL per well, 20 μL per well of lysis buffer and 10 μL per well of antibodies diluted in NaH$_2$PO$_4$ (50 mM) pH 7.4, NaF (400 mM), BSA (0.1%), and Tween 20 (0.05%)]. After incubation (30 min, room temperature), lysates were transferred to low-volume black-bottom 96-well plates, and Htt was determined after 3 h at 4 °C by time-resolved fluorescence with use of an EnVision® reader (Perkin–Elmer). Total protein in cell lysates was measured by use of the BCA-Protein detection kit (Perbio, Cramlington, UK).

Compound screen in 1536-well plate format: For the HTS format, the Htt573-Q72-expressing HN10 cells were incubated for three days with RSL-1 (400 nM) in DMEM and FCS (inducing medium,

10 %) to reach steady-state levels of mutant Htt expression. Htt-expressing cells (2000 cells per µL, 3 µL per well) were seeded in a 1536-microtiter plate (Greiner) and incubated overnight either in the absence or in the presence of compounds. When time-resolved FRET was multiplexed with resazurin cell viability readout, resazurin (2 µm) was added to the culture medium 4 h prior to the time-resolved FRET measurement. Resorufin levels were quantified after 4 h incubation at 580 nm excitation and 600 nm emission with an EnVision® reader (Perkin–Elmer). Afterwards, a sample buffer solution (5 µL per well) composed of three parts of lysis buffer [Triton X-100 (1 %) in PBS with Complete Protease Inhibitor] and two parts of antibody buffer [NaH_2PO_4 (50 mm) pH 7.4, NaF (400 mm), BSA (0.1 %), Tween 20 (0.05 %), K-labeled antibody (60 pg per well) and d2-labeled antibody (800 pg per well)] was added and the system was incubated for 30 min at room temperature. In some cases, plates were incubated at room temperature for longer times as indicated. Measurements were performed with a ViewLux™ device (Perkin–Elmer) with the following settings: Label 1 time-resolved FRET_Eu-K_(E:800K, Xsec, BF4, GN:high, SP:slow), Label 2 time-resolved FRET_XL665_(E:800K, Xsec, BF4, GN:high, SP:slow).

Data analysis: Time-resolved FRET measurement results in two different signals. After excitation at 320 nm, emission at 620 nm from the K-labeled antibody can be used as an internal reference for possible interfering artifacts of the assay such as signal quenching or absorption by compounds, sample turbidity, or differences in excitation energy or sample volume. The 665 nm emission signal originates from the d2 antibody, which is excited by time-resolved FRET when in proximity to the K antibody. The calculated 665/620 nm ratio is therefore an artifact-corrected specific signal of the two antibodies bound to the same polypeptide and hence a reflection of the amount of antigen protein present in the sample. For 96-well plate data, time-resolved FRET signals are given as the 665/620 nm ratio multiplied by 10 000.

For 1536-microtiter well plate optimization data, time-resolved signals are presented as ΔF values, a format more suitable for taking day-to-day assay variations into account as it is a background-corrected value [Eq. (1)]:

$$\Delta F = (\text{Ratio}_{665/620\,induced} - \text{Ratio}_{665/620\,noninduced}) / \text{Ratio}_{665/620\,noninduced} \times 100$$
(1)

Analysis of HTS data was conducted with the aid of in-house data analysis software. This software is able to normalize activity to percent remaining activity with the use of high and low control samples present on a plate and to correct for plate localization effects by use of a local regression algorithm.[29] Z'-factors were calculated according to ref. [30].

[1] G. P. Bates, P. Harper, L. Jones, *Huntington's Disease*, 3rd ed., Oxford University Press, Oxford, **2002**, pp. 28–94.

[2] The Huntington's Disease Collaborative Research Group, *Cell* **1993**, *72*, 971–983.

[3] G. Bates, *Lancet* **2003**, *361*, 1642–1644; G. P. Bates, E. Hockly, *Curr. Opin. Neurol.* **2003**, *16*, 465–470; G. P. Bates, C. Landles, *EMBO Rep.* **2004**, *5*, 958–963; A. B. Young, *J. Clin. Invest.* **2003**, *111*, 299–302.

[4] M. DiFiglia, M. Sena-Esteves, K. Chase, E. Sapp, E. Pfister, M. Sass, J. Yoder, P. Reeves, R. K. Pandey, *Proc. Natl. Acad. Sci. USA* **2007**, *104*, 17204–17209; Y. Machida, T. Okada, M. Kurosawa, F. Oyama, K. Ozawa, N. Nukina, *Biochem. Biophys. Res. Commun.* **2006**, *343*, 190–197; E. Rodriguez-Lebron, E. M. Denovan-Wright, K. Nash, A. S. Lewin, R. J. Mandel, *Mol. Ther.* **2005**, *12*, 618–633; Y. L. Wang, W. Liu, E. Wada, M. Murata, K. Wada, I. Kanazawa, *Neurosci. Res.* **2005**, *53*, 241–249.

[5] A. Yamamoto, J. J. Lucas, R. Hen, *Cell* **2000**, *101*, 57–66.

[6] I. Sanchez, C. Mahlke, J. Yuan, *Nature* **2003**, *421*, 373–379.

[7] S. C. Warby, E. Y. Chan, M. Metzler, L. Gan, R. R. Singaraja, S. F. Crocker, H. A. Robertson, M. R. Hayden, *Hum. Mol. Genet.* **2005**, *14*, 1569–1577.

[8] R. K. Graham, Y. Deng, E. J. Slow, B. Haigh, N. Bissada, G. Lu, J. Pearson, J. Shehadeh, L. Bertram, Z. Murphy, *Cell* **2006**, *125*, 1179–1191; C. L. Wellington, L. M. Ellerby, C. A. Gutekunst, D. Rogers, S. Warby, R. K. Graham, O. Loubser, J. van Raamsdonk, R. Singaraja, Y. Z. Yang, *J. Neurosci.* **2002**, *22*, 7862–7872.

[9] S. W. Davies, M. Turmaine, B. A. Cozens, M. DiFiglia, A. H. Sharp, C. A. Ross, E. Scherzinger, E. E. Wanker, L. Mangiarini, G. P. Bates, *Cell* **1997**, *90*, 537–548.

[10] B. Ravikumar, R. Duden, D. C. Rubinsztein, *Hum. Mol. Genet.* **2002**, *11*, 1107–1117.

[11] G. Mathis, *Clin. Chem.* **1993**, *39*, 1953–1959.

[12] H. Bazin, M. Preaudat, E. Trinquet, G. Mathis, *Spectrochim. Acta A. Mol. Biomol. Spectrosc.* **2001**, *57*, 2197–2211.

[13] P. E. Imbert, V. Unterreiner, D. Siebert, H. Gubler, C. Parker, D. Gabriel, *Assay Drug Dev. Technol.* **2007**, *5*, 363–372.

[14] D. Gabriel, M. Vernier, M. J. Pfeifer, B. Dasen, L. Tenaillon, R. Bouhelal, *Assay Drug Dev. Technol.* **2003**, *1*, 291–303.

[15] S. Achard, A. Jean, D. Lorphelin, M. Amoravain, E. J. Claret, *Assay Drug Dev. Technol.* **2003**, *1*, 181–185.

[16] S. M. Riddle, K. L. Vedvik, G. T. Hanson, K. W. Vogel, *Anal. Biochem.* **2006**, *356*, 108–116.

[17] N. J. Hassan, S. Gul, F. Flett, E. Hollingsworth, A. A. Dunne, A. J. Emmons, J. P. Hutchinson, M. J. Hibbs, S. Dyos, J. D. Kitson, E. Hiley, M. Ruediger, D. G. Tew, D. J. Powell, M. A. Morse, *Biochem. J.* **2009**, *419*, 65–73.

[18] E. E. Clarke, M. S. Shearman, *J. Neurosci. Methods* **2000**, *102*, 61–68.

[19] R. M. Clegg, *Fluorescence Imaging Spectroscopy and Microscopy*, Wiley, New York, **1996**, pp. 179–252; T. Förster, *Ann. Phys.* **1948**, *437*, 55–75.

[20] J. O'Brien, I. Wilson, T. Orton, F. Pognan, *Eur. J. Biochem.* **2000**, *267*, 5421–5426.

[21] J. Gafni, E. Hermel, J. E. Young, C. L. Wellington, M. R. Hayden, L. M. Ellerby, *J. Biol. Chem.* **2004**, *279*, 20211–20220.

[22] S. De Schepper, H. Bruwiere, T. Verhulst, U. Steller, L. Andries, W. Wouters, M. Janicot, J. Arts, J. Van Heusden, *J. Pharmacol. Exp. Ther.* **2003**, *304*, 881–888; N. Nishino, B. Jose, R. Shinta, T. Kato, Y. Komatsu, M. Yoshida, *Bioorg. Med. Chem.* **2004**, *12*, 5777–5784; M. Yoshida, S. Horinouchi, T. Beppu, *Bioassays* **1995**, *17*, 423–430.

[23] B. S. Baliga, A. W. Pronczuk, H. N. Munro, *J. Biol. Chem.* **1969**, *244*, 4480–4489; A. P. Grollman, *J. Biol. Chem.* **1967**, *242*, 3226–3233; G. Nass, *Zentralbl. Bakteriol.* **1970**, *212*, 239–245.

[24] N. Yamamoto, K. Takeshita, M. Shichijo, T. Kokubo, M. Sato, K. Nakashima, M. Ishimori, H. Nagai, Y. F. Li, T. Yura, K. B. Bacon, *J. Pharmacol. Exp. Ther.* **2003**, *306*, 1174–1181.

[25] S. Chen, V. Berthelier, W. Yang, R. Wetzel, *J. Mol. Biol.* **2001**, *311*, 173–182; S. Chen, F. A. Ferrone, R. Wetzel, *Proc. Natl. Acad. Sci. USA* **2002**, *99*, 11884–11889; W. Yang, J. R. Dunlap, R. B. Andrews, R. Wetzel, *Hum. Mol. Genet.* **2002**, *11* , 2905–2917.

[26] C. A. Gutekunst, S. H. Li, H. Yi, J. S. Mulroy, S. Kuemmerle, R. Jones, D. Rye, R. J. Ferrante, S. M. Hersch, X. J. Li, *J. Neurosci.* **1999**, *19*, 2522–2534; E. C. Stack, J. K. Kubilus, K. Smith, K. Cormier, S. J. Del Signore, E. Guelin, H. Ryu, S. M. Hersch, R. J. Ferrante, *J. Comp. Neurol.* **2005**, *490*, 354–370.

[27] P. A. Paganetti, M. Lis, H. W. Klafki, M. Staufenbiel, *J. Neurosci. Res.* **1996**, *46*, 283–293; A. Weihofen, M. K. Lemberg, E. Friedmann, H. Rueeger, A. Schmitz, P. Paganetti, G. Rovelli, B. Martoglio, *J. Biol. Chem.* **2003**, *278*, 16528–16533.

[28] H. J. Lee, D. N. Hammond, T. H. Large, B. H. Wainer, *Brain Res. Dev. Brain. Res.* **1990**, *52*, 219–228.

[29] H. Gubler, *Methods and Principles in Medicinal Chemistry, Vol. 28*, Wiley InterScience, New York, **2006**, pp. 151–205.

[30] J. H. Zhang, T. D. Chung, K. R. Oldenburg, *J. Biomol. Screening* **1999**, *4*, 67–73.